Letters

Direct Power Control Based on Natural Switching Surface for Three-Phase PWM Rectifiers

Junjie Ge, *Student Member, IEEE*, Zhengming Zhao, *Senior Member, IEEE*, Liqiang Yuan, *Member, IEEE*, Ting Lu, *Member, IEEE*, and Fanbo He, *Member, IEEE*

***Abstract*—In this letter, the natural trajectories of the output voltage and the inductor currents for three-phase pulse width modulation rectifiers are presented. On this basis, a novel direct power control (DPC) using the natural switching surface is proposed by combining DPC with the boundary control. Compared to the conventional DPC, the proposed control considers the output voltage when selecting the switching states. Therefore, the proposed control does not need an outer voltage control loop and can highly improve the dynamic performance of the dc output voltage. The experimental results on a 1.5-kW prototype confirm the correctness of the theoretical analysis. They verify the feasibility and the validity of the proposed control and show the excellent dynamic performance.**

***Index Terms*—Boundary control, direct power control (DPC), natural trajectory, switching surface, three-phase pulse width modulation (PWM) rectifier.**

I. Introduction

BOUNDARY control, which is a geometric based control method, is suitable for power electronic converters with switching actions [1], [2]. It has been applied in many converters, and there are a variety of studies on different switching surfaces, e.g., first-order, second-order, and high-order switching surfaces [3]–[6]. Among them, the natural switching surfaces show quite good dynamic performance. Papers [7]–[11] present boundary control schemes for buck converters, boost converters, single-phase power factor correctors, single inverters, and dual-active bridge converters using the natural switching surface, which provides excellent transient behavior and no overshoot. However, these papers only study the applications in the converters, which have one inductor current. There are a little related literatures published about the natural trajectories of three-phase pulse width modulation (PWM) rectifiers, which have three inductor currents and need a more complex boundary control. Paper [12] studies the natural switching surface of three-phase currents, but not the natural switching surface of the inductor currents and the output voltage. Therefore, the proposed control method can quickly regulate the input currents, but not the output voltage.

Direct power control (DPC), which uses the instantaneous active and reactive power to control the power converter is one of most efficient control strategies for three-phase PWM rectifiers [13]–[16]. The switching states are selected by a switching table based on the instantaneous power errors and the input voltage vector position. By using new switching tables, adaptive control, fuzzy logic selection, sliding mode, duty-cycle optimization, or predictive method, studies on DPC can cope with parameter uncertainties, enhance disturbance rejection ability, improve steady-state performance, simplify the control, etc., [17]–[23]. However, their improvement on the dynamic performance of the dc output voltage is limited. Since DPC is easy to implement and has the behavior of bang–bang control, it can be combined with the boundary control to achieve the excellent dynamic performance of the dc output voltage.

This letter proposes a novel DPC based on the natural switching surface for three-phase PWM rectifiers by combining DPC with the boundary control. For ease of study, the mathematical model in *dq* coordinates is set up first. On this basis, the natural trajectories of the inductor currents and the output voltage with different states are presented and analyzed. Then, employing DPC and taking the natural trajectories as switching surfaces, the proposed control is realized. Compared to the conventional applications [7]–[12], this letter expands natural switching surface into the three-phase converters, and employs it to regulate the output voltage with DPC. Different from the conventional DPC, the proposed DPC does not have an outer voltage-control loop and has a novel way to select switching states. An excellent dynamic performance of the dc output voltage can be achieved by the proposed control. At last, the experimental results, which are in agreement with the theoretical analysis, are provided to verify the proposed control.

II. Mathematical Model of Three-Phase Rectifiers

The configuration of three-phase PWM rectifiers is shown in Fig. 1, where L is the inductor, $R_{\rm g}$ is the inductor resistance, C is the capacitor, $\rm S_a - S_c$ are the switches, $e_{\rm a} - e_{\rm c}$ are the three-phase input voltages, $i_{L\rm a} - i_{L\rm c}$ are the three-phase inductor currents, u_C is the capacitor voltage, i.e., output voltage, and $i_{\rm O}$ is the output current.

Manuscript received October 7, 2014; revised October 30, 2014; accepted November 22, 2014. Date of publication December 4, 2014; date of current version January 16, 2015.

The authors are with the State Key Laboratory of Power System, Department of Electrical Engineering, Tsinghua University, Beijing 100084, China (e-mail: gejunjie1359@163l.com; zhaozm@tsinghua.edu.cn; ylq@tsinghua.edu.cn; lut@mails.tsinghua.edu.cn; hefanbo@gmail.com).

Color versions of one or more of the figures in this paper are available online at http://ieeexplore.ieee.org.

Digital Object Identifier 10.1109/TPEL.2014.2377048

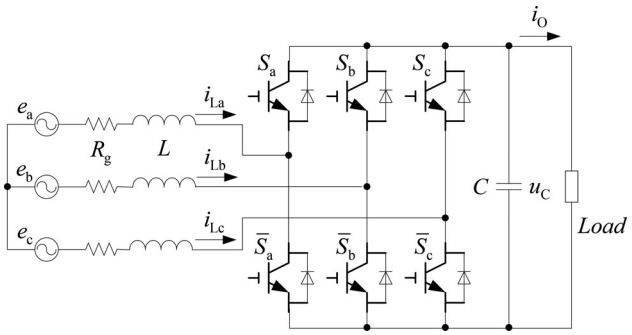

Fig. 1. Configuration of three-phase PWM rectifiers.

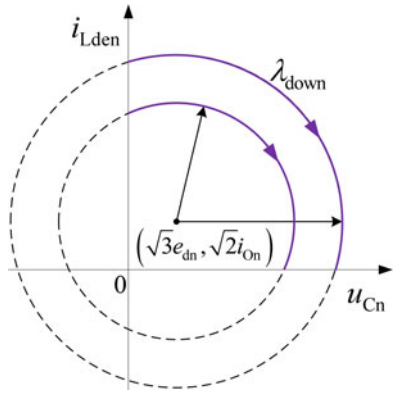

Fig. 2. Natural trajectory with current decrease.

In synchronous rotating coordinates (i.e., *dq* coordinates), the *d*-axis and the *q*-axis components of the input voltage through *dq* transform are e_{d} and e_{q}, respectively. Similarly, the *d*-axis and the *q*-axis components of the inductor currents are i_{Ld} and i_{Lq}. The mathematical model of three phase PWM rectifiers in *dq* coordinates is set up as

$$\begin{cases} L\dfrac{di_{Ld}}{dt} = -R_{\mathrm{g}}i_{Ld} + \omega L i_{Lq} + e_{\mathrm{d}} - u_{\mathrm{Sd}} \\ L\dfrac{di_{Lq}}{dt} = -R_{\mathrm{g}}i_{Lq} - \omega L i_{Ld} + e_{\mathrm{q}} - u_{\mathrm{Sq}} \\ C\dfrac{du_C}{dt} = \dfrac{3\left(u_{\mathrm{Sd}}i_{Ld} + u_{\mathrm{Sq}}i_{Lq}\right)}{2u_C} - i_{\mathrm{O}} \end{cases} \tag{1}$$

where ω is the rotating speed, u_{Sd} and u_{Sq} are the *d*-axis and the *q*-axis components of the converter voltage.

Generally, e_{q} is zero and i_{Lq} is controlled to be zero for unity power fact. When R_{g} is small enough to be ignored, the simplified model can be obtained as

$$\begin{cases} L\dfrac{di_{Ld}}{dt} = e_{\mathrm{d}} - u_{\mathrm{Sd}} \\ C\dfrac{du_C}{dt} = \dfrac{3u_{\mathrm{Sd}}}{2u_C}i_{Ld} - i_{\mathrm{O}}. \end{cases} \tag{2}$$

III. Natural Trajectories

With different converter voltages, the inductor currents and the capacitor voltage have the different natural trajectories in the phase plane. The natural trajectories of current decrease and increase will be investigated in the following.

According to the principle of converter control, the maximum value of u_{sd} is

$$u_{\mathrm{Sd\_max}} = \pm\frac{u_C}{\sqrt{3}}. \tag{3}$$

For ease of discussion, a simple normalization will be done as follows:

$$u_{C\mathrm{n}} = u_C \tag{4}$$

$$i_{L\mathrm{n}} = \sqrt{\frac{L}{C}}i_L. \tag{5}$$

A. Natural Trajectory of Current Decrease

When decreasing the current, u_{sd} should be the positive value as

$$u_{\mathrm{Sd}} = \frac{u_C}{\sqrt{3}}. \tag{6}$$

From (2) and (6), there are

$$\begin{cases} \sqrt{2}L\dfrac{di_{L\mathrm{de}}}{dt} = \sqrt{3}e_{\mathrm{d}} - u_C \\ \sqrt{2}C\dfrac{du_C}{dt} = i_{L\mathrm{de}} - \sqrt{2}i_{\mathrm{O}}. \end{cases} \tag{7}$$

where

$$i_{L\mathrm{de}} = \sqrt{\frac{3}{2}}i_{Ld}. \tag{8}$$

Using the similar derivation method in [8], (7) can be rewritten as

$$L\left(i_{L\mathrm{de}} - \sqrt{2}i_{\mathrm{O}}\right)^2 + C\left(u_C - \sqrt{3}e_{\mathrm{d}}\right)^2 = m^2. \tag{9}$$

where *m* is a constant that is related to the initial values of $i_{L\mathrm{de}}$ and u_C.

Substituting (4) and (5) into (9), the natural trajectory of current decrease λ_{down} is given as

$$\left(i_{L\mathrm{den}} - \sqrt{2}i_{\mathrm{On}}\right)^2 + \left(u_{Cn} - \sqrt{3}e_{\mathrm{dn}}\right)^2 = h^2 \tag{10}$$

where *h* is the radius and $e_{\mathrm{dn}} = e_{\mathrm{d}}, i_{\mathrm{On}} = \sqrt{\frac{L}{C}}i_{\mathrm{O}}$. In the normalized phase plane, λ_{down} are circles with the center on $\left(\sqrt{3}e_{\mathrm{dn}}, \sqrt{2}i_{\mathrm{On}}\right)$, as shown in Fig. 2.

B. Natural Trajectory of Current Increase

When increasing the current, u_{sd} should be the negative value as

$$u_{\mathrm{Sd}} = -\frac{u_C}{\sqrt{3}}. \tag{11}$$

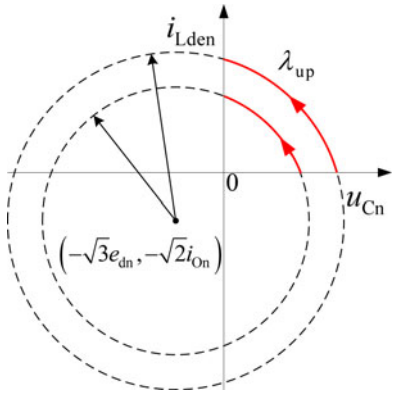

Fig. 3. Natural trajectory with current increase.

From (2), (8), and (11), there are

$$\begin{cases} \sqrt{2}L\dfrac{di_{L\mathrm{de}}}{dt} = \sqrt{3}e_{\mathrm{d}} + u_C \\ \sqrt{2}C\dfrac{du_C}{dt} = i_{L\mathrm{de}} + \sqrt{2}i_{\mathrm{O}}. \end{cases} \tag{12}$$

Using the similar derivation method in [8], (12) can be rewritten as

$$L\left(i_{L\mathrm{de}} + \sqrt{2}i_{\mathrm{O}}\right)^2 + C\left(u_{\mathrm{C}} + \sqrt{3}e_{\mathrm{d}}\right)^2 = n^2 \tag{13}$$

where n is a constant that is related to the initial values of $i_{L\mathrm{de}}$ and u_C as well.

Substituting (4) and (5) into (13), the natural trajectory of current increase λ_{up} is given as

$$\left(i_{L\mathrm{den}} + \sqrt{2}i_{\mathrm{On}}\right)^2 + \left(u_{C\mathrm{n}} + \sqrt{3}e_{\mathrm{dn}}\right)^2 = l^2 \tag{14}$$

where l is the radius. Similarly, λ_{up} are circles with the center on $\left(-\sqrt{3}e_{\mathrm{dn}}, -\sqrt{2}i_{\mathrm{On}}\right)$ in the normalized phase plane, as shown in Fig. 3.

IV. DPC Based on Natural Switching Surface

DPC, which is easy to implement for three-phase PWM rectifiers and has the behavior of bang–bang control, can be combined with the boundary control to improve the dynamic performance of the dc output voltage. Employing DPC and taking the natural trajectories above as switching surfaces, a novel DPC which considers the output voltage when selecting the switching states is proposed.

Since only the active power impacts on the dc output voltage and the change of instantaneous active power p_{n} is the change of $i_{L\mathrm{den}}$, the switching state changing p_{n} can be used to regulate the operation trajectory. The control laws of the proposed control are in the following. Define

$$R_{\mathrm{T\_down}} = \sqrt{\left(i_{L\mathrm{den\_T}} - \sqrt{2}i_{\mathrm{On}}\right)^2 + \left(u_{C\mathrm{n\_T}} - \sqrt{3}e_{\mathrm{dn}}\right)^2} \tag{15}$$

TABLE I
Switching Table

S_{p}	S_{q}	θ_1	θ_2	θ_3	θ_4	θ_5	θ_6	θ_7	θ_8	θ_9	θ_{10}	θ_{11}	θ_{12}
1	0	v_6	v_7	v_1	v_0	v_2	v_7	v_3	v_0	v_4	v_7	v_5	v_0
	1	v_7	v_7	v_0	v_0	v_7	v_7	v_0	v_0	v_7	v_7	v_0	v_0
0	0	v_6	v_1	v_1	v_2	v_2	v_3	v_3	v_4	v_4	v_5	v_5	v_6
	1	v_1	v_2	v_2	v_3	v_3	v_4	v_4	v_5	v_5	v_6	v_6	v_1

v_1 (100), v_2 (110), v_3 (010), v_4 (011), v_5 (001), v_6 (101), v_0 (000), v_7 (111).

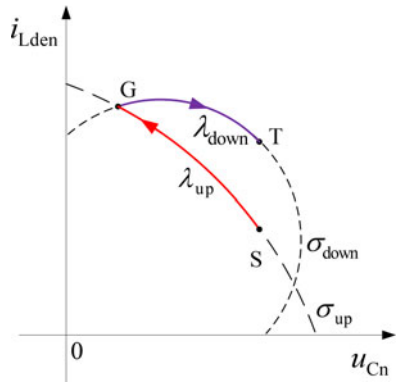

Fig. 4. Natural switching surface for DPC.

$$R_{\mathrm{T\_up}} = \sqrt{\left(i_{L\mathrm{den\_T}} + \sqrt{2}i_{\mathrm{On}}\right)^2 + \left(u_{C\mathrm{n\_T}} + \sqrt{3}e_{\mathrm{dn}}\right)^2} \tag{16}$$

where $u_{C\mathrm{n\_T}}$ and $i_{L\mathrm{den\_T}}$ are the voltage and current of the target operation point.

The natural switching surfaces according to λ_{down} and λ_{up} are selected as

$$\sigma_{\mathrm{down}} = \left(i_{L\mathrm{den}} - \sqrt{2}i_{\mathrm{On}}\right)^2 + \left(u_{C\mathrm{n}} - \sqrt{3}e_{\mathrm{dn}}\right)^2 - R^2_{\mathrm{T\_down}} \tag{17}$$

$$\sigma_{\mathrm{up}} = \left(i_{L\mathrm{den}} + \sqrt{2}i_{\mathrm{On}}\right)^2 + \left(u_{C\mathrm{n}} + \sqrt{3}e_{\mathrm{dn}}\right)^2 - R^2_{\mathrm{T\_up}}. \tag{18}$$

In the novel DPC, the digitized signals S_{q} and the switching table are the same as the conventional DPC [13]–[15]. Only the digitized signals S_{p} is obtained in a different way based on the natural switching surfaces as

Case I: $u_C < u_{C\_\mathrm{T}}$

$$\text{If } \sigma_{\mathrm{down}} < 0, \text{ then } S_{\mathrm{p}} = 1, \text{else } S_{\mathrm{p}} = 0. \tag{19}$$

Case II: $u_C > u_{C\_\mathrm{T}}$

$$\text{If } \sigma_{\mathrm{up}} > 0, \text{ then } S_{\mathrm{p}} = 0, \text{else } S_{\mathrm{p}} = 1. \tag{20}$$

Since the digitized signals S_{q} is obtained as

$$S_{\mathrm{q}} = \begin{cases} 1, & q < q_{\mathrm{r}} - H_{\mathrm{q}} \\ 0, & q > q_{\mathrm{r}} + H_{\mathrm{q}} \end{cases} \tag{21}$$

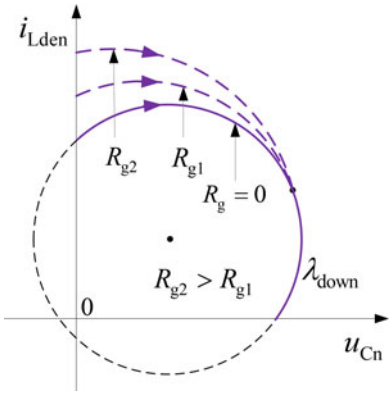

Fig. 5. Trajectories with different inductor resistances.

TABLE II
PARAMETERS OF EXPERIMENTAL CIRCUIT

Parameter	Value
Input phase voltage e	48 V
Output voltage u_C	120 V
Inductor L	2.6 mH
Inductor resistance R_g	0.28 Ω
Capacitor C	2350 μF

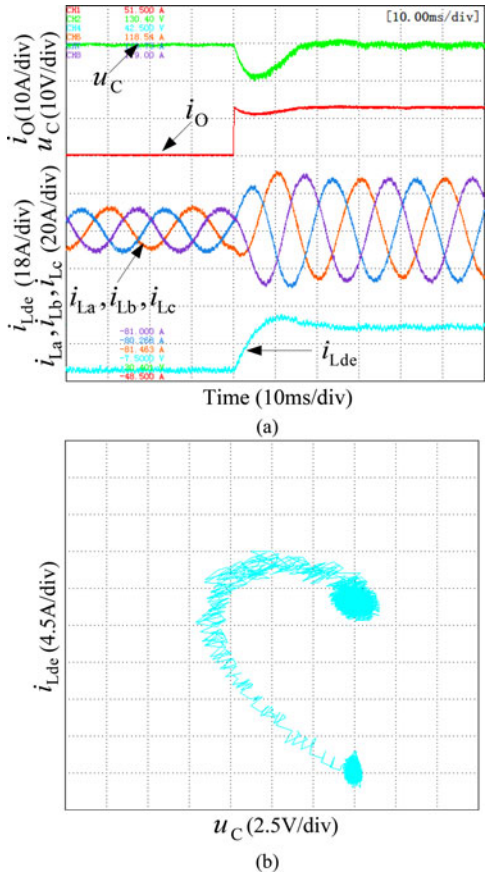

Fig. 6. Experimental waveforms of conventional DPC. (a) Capacitor voltage, output current, three-phase inductor currents, and d-axis inductor current. (b) Phase plane.

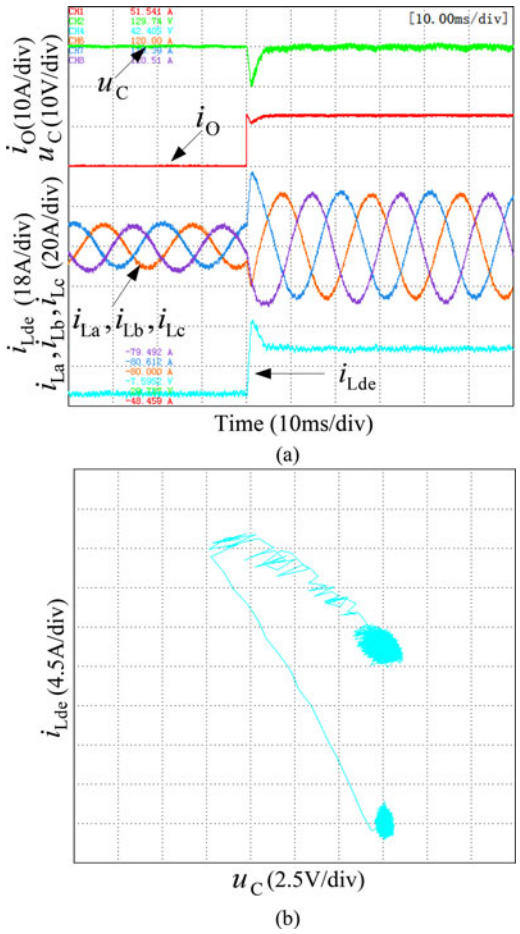

Fig. 7. Experimental waveforms of the proposed control. (a) Capacitor voltage, output current, three-phase inductor currents, and d-axis inductor currents. (b) Phase plane.

where q is the instantaneous reactive power, q_r is the target reactive power, and H_q is the hysteresis band of reactive power, the switching states can be selected by Table I based on (19)–(21).

As shown in Fig. 4, the operation trajectory in DPC based on the natural switching surface when the load suddenly increases will be around the natural trajectories. It can achieve the effect of boundary control and complete the transition process in a very short time.

If R_g is not zero, the natural trajectories will be a little different. As shown in Fig. 5, the larger the R_g is, the farther the real natural trajectory leaves the trajectory with $R_g = 0$. Since the expression of the natural trajectory with $R_g \neq 0$ is difficult to solve for control, the natural switching surface with $R_g = 0$ can still be used to guarantee no overshoot.

V. EXPERIMENTAL RESULTS

In order to verify the theoretical analysis and the validity of the proposed control, a three-phase PWM rectifier prototype of 1.5 kW is established. The digital-signal-processor TMS320F28335, which samples at 40 kHz is utilized for the

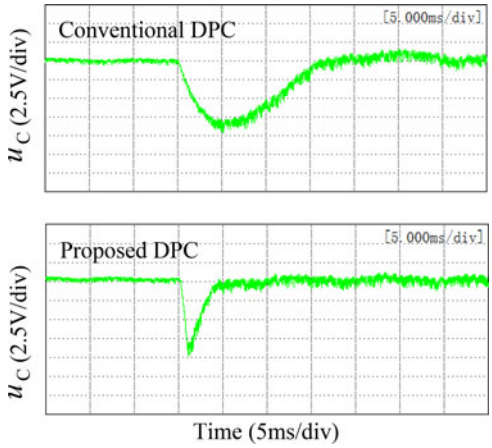

Fig. 8. Dynamic performances of the dc output voltage.

experiments. Thus, the maximum switching frequency is 20 kHz, but the average frequency is much lower, only about 6.4 kHz when H_q is zero. The parameters of the experimental circuit are listed in Table II.

When the load suddenly changes from 20 to 10 Ω, the experimental waveforms of the conventional DPC are shown in Fig. 6, and the experimental waveforms of the proposed control are shown in Fig. 7. As can be seen, their steady-state performances both are quite good. However, their transition processes and trajectories are different from each other. As shown in Fig. 7(b), the phase-plane trajectory of the proposed control is around the natural trajectories, which is in agreement with the theoretical analysis. Compared to the conventional DPC, the proposed control can highly improve the dynamic performance of the dc output voltage with a shorter transition time, as shown in Fig. 8.

VI. Conclusion

This letter combines DPC with boundary control and proposes a novel DPC based on the natural switching surface for three-phase PWM rectifiers. The natural trajectories of the *d*-axis inductor current and the capacitor voltage are derived and studied based on the mathematical model in *dq* coordinates. The proposed DPC takes the natural trajectories as switching surfaces and achieves the effect of the boundary control. It can highly improve the dynamic performance of the dc output voltage. The experimental results on a 1.5-kW prototype verify the validity of the proposed control.

Acknowledgment

The authors would like to thank the State Grid Corporation of China for the support of the project titled Research on the Energy Router in the Distribution Network for the Energy Internet.

References

[1] R. Munzert and P. T. Krein, "Issues in boundary control," in *Proc. IEEE Power Electron. Spec. Conf.*, 1996, pp. 810–816.
[2] M. Greuel, R. Muyshondt, and P. T. Krein, "Design approaches to boundary controllers," in *Proc. IEEE Power Electron. Spec. Conf.*, 1997, pp. 672–678.
[3] C. N. Onwuchekwa and A. Kwasinski, "Analysis of boundary control for buck converters with instantaneous constant-power loads," *IEEE Trans. Power Electron.*, vol. 25, no. 8, pp. 2018–2032, Aug. 2010.
[4] S. Chen, M. Yuk, S. Tan, and K. Chi, "Boundary control with ripple-derived switching surface for DC-AC inverters," *IEEE Trans. Power Electron.*, vol. 24, no. 12, pp. 2873–2885, Dec. 2009.
[5] K. K. Leung and H. S. Chung, "A comparative study of boundary control with first- and second-order switching surfaces for buck converters operating in DCM," *IEEE Trans. Power Electron.*, vol. 22, no. 4, pp. 1196–1209, Jul. 2007.
[6] J. Y. Chiu, K. K. Leung, and H. S. Chung, "High-order switching surface in boundary control of inverters," *IEEE Trans. Power Electron.*, vol. 22, no. 5, pp. 1753–1765, Sep. 2007.
[7] M. Ordonez, M. T. Iqbal, and J. E. Quaicoe, "Selection of a curved switching surface for buck converters," *IEEE Trans. Power Electron.*, vol. 21, no. 4, pp. 1148–1153, Jul. 2006.
[8] J. Galvez, M. Ordonez, F. Luchino, and J. Quaicoe, "Improvements in boundary control of boost converters using the natural switching surface," *IEEE Trans. Power Electron.*, vol. 26, no. 11, pp. 3367–3376, Nov. 2011.
[9] J. M. Galvez and M. Ordonez, "High performance boundary control of boost-derived PFCs: Natural switching surface derivation and properties," *IEEE Trans. Power Electron.*, vol. 27, no. 8, pp. 3807–3816, Aug. 2012.
[10] M. Ordonez, J. E. Quaicoe, and M. T. Iqbal, "Advanced boundary control of inverters using the natural switching surface: Normalized geometrical derivation," *IEEE Trans. Power Electron.*, vol. 23, no. 6, pp. 2915–2930, Nov. 2008.
[11] G. Oggier, M. Ordonez, J. Galvez, and F. Luchino, "Fast transient boundary control and steady-state operation of the dual active bridge converter using the natural switching surface," *IEEE Trans. Power Electron.*, vol. 29, no. 2, pp. 946–957, Feb. 2014.
[12] J. M. Galvez and M. Ordonez, "Introducing the natural switching surface for reference frame systems: Three-phase boost PFCs," in *Proc. IEEE Energy Convers. Congr. Expo.*, 2012, pp. 1064–1070.
[13] H. Akagi, Y. Kanazawa, and A. Nabae, "Instantaneous reactive power compensators comprising switching devices without energy storage," *IEEE Trans. Ind. Appl.*, vol. IA-20, no. 3, pp. 625–630, May/Jun. 1984.
[14] T. Noguchi, H. Tomiki, S. Kondo, and I. Takahashi, "Direct power controlof PWM converter without power-source voltage sensors," *IEEE Trans. Ind. Appl.*, vol. 34, no. 3, pp. 473–479, May/Jun. 1998.
[15] G. Escobar, A. Stankovic, J. M. Carrasco, E. Galvan, and R. Ortega, "Analysis and design of direct power control (DPC) for a three phase synchronous rectifier via output regulation subspaces," *IEEE Trans. Power Electron.*, vol. 18, no. 3, pp. 823–830, May 2003.
[16] M. Malinowski, M. Jasinski, and M. P. Kazmierkowski, "Simple direct power control of three-phase PWM rectifier using space-vector modulation (DPC-SVM)," *IEEE Trans. Ind. Electron.*, vol. 51, no. 2, pp. 447–454, Apr. 2004.
[17] S. Vazquez, J. A. Sanchez, J. M. Carrasco, J. I. Leon, and E. Galvan, "A model-based direct power control for three-phase power converters," *IEEE Trans. Ind. Electron.*, vol. 55, no. 4, pp. 1647–1657, Apr. 2008.
[18] P. R. Martinez-Rodriguez, G. Escobar, A. A. Valdez-Fernandez, M. Hernandez-Gomez, and J. M. Sosa, "Direct power control of a three-phase rectifier based on positive sequence detection," *IEEE Trans. Ind. Electron.*, vol. 61, no. 8, pp. 4084–4092, Aug. 2014.
[19] A. Bouafia, F. Krim, and J. Gaubert, "Fuzzy-logic-based switching state selection for direct power control of three-phase PWM rectifier," *IEEE Trans. Ind. Electron.*, vol. 56, no. 6, pp. 1984–1992, Jun. 2009.
[20] H. Jingjing, Z. Aimin, Z. Hang, R. Zhigang, W. Jianhua, Z. Lei, and Z. Chao, "Improved direct power control for rectifier based on Fuzzy sliding mode," *IEEE Trans. Control Syst. Technol.*, vol. 22, no. 3, pp. 1174–1180, May 2014.
[21] Z. Yongchang, X. Wei, L. Zhengxi, and Z. Yingchao, "Model predictive direct power control of a PWM rectifier with duty cycle optimization," *IEEE Trans. Power Electron.*, vol. 28, no. 11, pp. 5343–5351, Nov. 2013.
[22] Z. Yongchang, L. Zhengxi, Z. Yingchao, X. Wei, P. Zhengguo, and H. Changbin, "Performance improvement of direct power control of PWM rectifier with simple calculation," *IEEE Trans. Power Electron.*, vol. 28, no. 7, pp. 3428–3437, Jul. 2013.
[23] A. Bouafia, J. Gaubert, and F. Krim, "Predictive direct power control of three-phase pulsewidth modulation (PWM) rectifier using space-vector modulation (SVM)," *IEEE Trans. Power Electron.*, vol. 25, no. 1, pp. 228–236, Jan. 2010.